



Aalborg Universitet

AALBORG UNIVERSITY  
DENMARK

## Multi-Connectivity for Ultra-Reliable Communication in Industrial Scenarios

Khatib, Emil Jatib; Assefa, Dereje; Berardinelli, Gilberto; Rodriguez, Ignacio; Mogensen, Preben Elgaard

*Published in:*  
2019 IEEE 89th Vehicular Technology Conference (VTC2019-Spring)

*DOI (link to publication from Publisher):*  
[10.1109/VTCSpring.2019.8746357](https://doi.org/10.1109/VTCSpring.2019.8746357)

*Publication date:*  
2019

*Document Version*  
Accepted author manuscript, peer reviewed version

[Link to publication from Aalborg University](#)

*Citation for published version (APA):*  
Khatib, E. J., Assefa, D., Berardinelli, G., Rodriguez, I., & Mogensen, P. E. (2019). Multi-Connectivity for Ultra-Reliable Communication in Industrial Scenarios. In *2019 IEEE 89th Vehicular Technology Conference (VTC2019-Spring)* [8746357] IEEE. IEEE Vehicular Technology Conference. Proceedings  
<https://doi.org/10.1109/VTCSpring.2019.8746357>

### General rights

Copyright and moral rights for the publications made accessible in the public portal are retained by the authors and/or other copyright owners and it is a condition of accessing publications that users recognise and abide by the legal requirements associated with these rights.

- ? Users may download and print one copy of any publication from the public portal for the purpose of private study or research.
- ? You may not further distribute the material or use it for any profit-making activity or commercial gain
- ? You may freely distribute the URL identifying the publication in the public portal ?

### Take down policy

If you believe that this document breaches copyright please contact us at [vbn@aub.aau.dk](mailto:vbn@aub.aau.dk) providing details, and we will remove access to the work immediately and investigate your claim.

# Multi-Connectivity for Ultra-Reliable Communication in Industrial Scenarios

Emil J. Khatib\*, Dereje Assefa Wassie\*, Gilberto Berardinelli\*, Ignacio Rodriguez\*, Preben Mogensen\*

\* *Wireless Communication Networks*

*Aalborg University, Denmark*

{ejk, daw, gb, irl, pm}@es.aau.dk

**Abstract**—In the last years, wireless communications in industrial scenarios are becoming an increasingly important market. Some of these communications have tight reliability requirements, but harsh propagation conditions in industrial scenarios represent a major challenge. In this paper, multi-connectivity is explored as a solution for assuring high reliability in industrial scenarios. Several multi-connectivity techniques are compared, using real channel measurements from two factories. Multi-connectivity comes at the cost of a reduced throughput in the mobile broadband services on the same network. In this paper, this impact is quantified to assess for the cost of implementing multi-connectivity.

**Index Terms**—industrial communication, reliability, multi-connectivity, MRC, IRC

## I. INTRODUCTION

In the last decades, industrial processes have undergone a new revolution with the Industry 4.0 paradigm [1] and the Internet of Things [2]. Telecommunication technologies and, more specifically, wireless data networks play a central role in these technological trends. The new cellular network generations, such as 5G, offer a competitive alternative to wired networks in the industry, allowing for an agile deployment and reduced installation complexity and costs.

The development of 5G takes into account the requirements of industrial communication. Specifically, two main communication profiles are supported [3]:

- Massive Machine Type Communications (MMTC): it represents non mission-critical messages coming from a large number of sources. Typically used by sensors that monitor a process continuously.
- Ultra Reliable Low Latency Communications (URLLC): mission-critical messages that require a very high reliability and a low latency. Used for alarms, special events measured by sensors for a closed loop control.

These two Machine Type Communication (MTC) profiles are complemented with Enhanced Mobile Broadband (eMBB), which is commonly associated with personal communications, but that also has its use in industrial scenarios, for instance in surveillance video feeds.

In order to accommodate the requirements of these communication profiles, a large network capacity is required. In previous generations, cell densification was exploited to increase the network capacity [4]. In the upcoming 5G network, this trend will continue. It is expected that in geographical areas where the number of devices is higher, or the requirements are

more stringent, small cell deployments will increase network capacity. This is precisely the case for the industrial scenarios where a large number of MTC devices will be deployed. A massive number of small cells will support not only a higher capacity, but also the tight reliability requirements of industrial communications. However, cell densification suffers from an increased level of interference. To deal with this, several interference mitigation techniques such as inter-cell interference coordination and advanced receivers have been used [5]. In particular, advanced receivers such as Interference Rejection Combining (IRC) have shown significant benefits in dense small cells deployments [6]. Besides the interference challenge, in industrial scenarios, harsh propagation conditions [7] are another limiting factor, for improving the capacity and fulfilling the tight reliability requirements of mission-critical services.

This paper focuses on the usage of multi-connectivity for improving the reliability in industrial scenarios [8]. In multi-connectivity, one User Equipment (UE) terminal may be connected to more than one Access Point (AP) simultaneously. It has been proposed, for instance, for increasing the capacity of a UE for eMBB services [9] or for ensuring connectivity at the cell edge [10]. In this paper, multi-connectivity is used for improving reliability by increasing the redundancy of data transmission.

Multi-connectivity can be analyzed via system level Monte Carlo simulations by reproducing a network of dense small cells. Nevertheless, standard propagation models may not fully capture the real propagation characteristics of a given scenario. For instance, the work in [11] indicated that commonly used path loss models such as WINNER II do not correctly predict the real measured path loss in indoor scenarios. This discrepancy will be further exacerbated in indoor industrial scenarios due to their specific characteristics, such as the presence of massive metallic machinery; therefore, a pure simulation study may not provide a realistic assessment of the advantages of using multi-connectivity techniques for mission-critical communications. Hence, in this paper, the performance of multi-connectivity is analyzed using a hybrid emulation approach where the channel models are superseded by real channel measurements. For this analysis, radio propagation measurements are run in two different factory scenarios using a Software Defined Radio (SDR) testbed [12].

The paper is structured as follows. Section II describes

how multi-connectivity can be used to enhance reliability, and the considered techniques. In Section III, the measurement process, as well as the hybrid emulation technique will be described, detailing the configuration parameters for the scenario. The results are shown and discussed in Section IV; and finally, in Section V, the conclusions are presented.

## II. MULTI-CONNECTIVITY FOR INDUSTRIAL ULTRA-RELIABLE COMMUNICATIONS

Typically, in wireless networks, a UE is served by a single AP. In multi-connectivity, a single UE may be connected simultaneously to more than one AP at a given time. In case the multiple serving links are spatially uncorrelated, multi-connectivity can provide the required diversity for compensating poor channel conditions. This is particularly important in harsh propagation scenarios, which is the case of industrial environments. In large factories with a large amount of heavy metallic structures, as well as concrete walls, shadowing is indeed the major limiting performance factor [7], and can jeopardize the possibility of establishing a reliable communication in case proper countermeasures are not taken into account.

Packet duplication is a multi-connectivity solution meant at improving reliability by increasing redundancy of the transmission [8]. When a packet reaches a certain AP which acts as primary node (PN), such packet is duplicated and transmitted to a secondary node (SN); both APs take care of transmitting the same packet to UEs demanding reliable communication. There are several ways to implement packet duplication in multi-connectivity, depending on the layer where the duplication is performed:

- Physical layer duplication: the APs coordinate at physical layer to transmit the packet. On the receiver side, the UE combines the received packet at physical layer, with the rest of the layers being agnostic to multi-connectivity. We consider two possibilities for physical layer duplication:
  - Single Frequency Network (SFN) [13] : the APs transmit simultaneously the same waveform over the same frequency resources. The UE will then receive the superposition of the same signal from several points. SFN exploits opportunistically constructive interference for boosting the power of the signal.
  - Joint Transmission (JT) [14]: the APs transmit simultaneously the same physical layer packet over the same or different frequency resources; however, the waveforms are multiplied by an AP-specific precoding matrix which is calculated upon the estimated channel matrix. Such scheme requires the channel knowledge at the transmitter, and allows for coherent receive combining with the promise of further strengthening the signal power. Note that we are not considering here the case of coherent JT known in literature (e.g., [15]), where the precoding matrices are designed according to shared channel state information among the APs, but each AP applies its precoding matrix individually according to its own channel. Further details on the scheme used in our

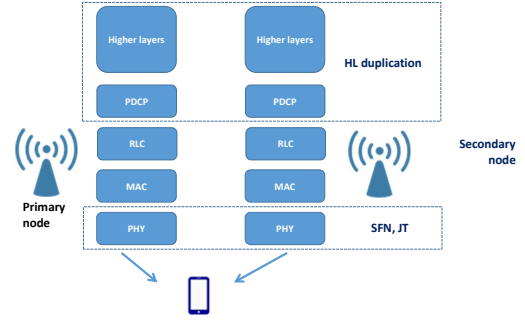


Fig. 1. Summary of the different packet duplication techniques

evaluation will be provided in the implementation section.

- Higher layer (HL) duplication [8]: the packet is duplicated at PDCP (Packet Data Convergence Protocol) layer or above (e.g. network via multi-path TCP [16], or application). The packet will then undergo independent Radio Link Control (RLC), Medium Access Control (MAC) and physical layer processing at each AP. As a consequence, the packet can eventually be transmitted at different time instants, over different frequency resources and with different physical layer parameters such as modulation and coding scheme (MCS). On the receiver side, the UE will receive the multiple versions of the same packet, and eventually discard replicas in case the packet has already been correctly received. Duplication at PDCP layer is studied by the 3GPP for its inclusion in 5G [17].

Figure 1 shows the distribution of the different packet duplication schemes over the network layers.

Physical layer duplication requires tight synchronization. In particular, when using OFDM, the synchronization error must be below the cyclic prefix duration of the symbols. Such tight synchronization needs a high capacity connection between the APs, which increases the costs of deployment. Higher layer duplication has more relaxed requirements in terms of backhaul connection since the duplicated packets are not to be transmitted simultaneously. On the other side, this may translate to a latency increase.

## III. EVALUATION

For evaluating multi-connectivity in industrial scenarios, a hybrid emulation approach is used. In this approach, the higher layers will be emulated, while the physical layer will use real channel measurements instead of standard channel models. It is worth to mention that in this paper we do not analyze latency aspects, whose study is left for future work.

The scenario that is emulated in this paper consists of 4 APs and 4 UEs, as shown in Figure 2. We assume that one of the 4 UEs is demanding reliable communication (RC), while the other 3 UEs are eMBB users. Our focus is on the downlink. An Open Subscriber Group (OSG) mode is assumed, where each UE connects to the AP for which it

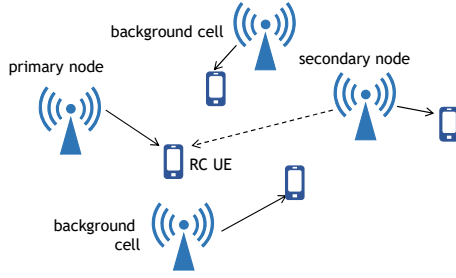


Fig. 2. Basic emulated scenario.

measures the highest receive signal power. We assume that the APs (either PN or SN) serving the RC UE do not serve other users. Conversely, the other APs can instead serve multiple eMBB UEs by equally dividing its transmission bandwidth. Frequency reuse one is assumed, i.e. each UE suffers from the interference generated by the APs not serving itself.

Two main Key Performance Indicators (KPIs) are extracted for performance assessment:

- Signal to Interference plus Noise Ratio (SINR) for the RC UE, calculated assuming different multi-antenna receiver types. Specifically, we consider a Maximum Ratio Combining (MRC) receiver, which exploits spatial diversity to boost the power of the received signal, and an Interference Rejection Combining (IRC) receiver, which is able to suppress the strongest interference sources. Both receivers exploit the degrees of freedom offered by multi-antenna reception to strengthen the power of the useful signal. A packet is correctly received in case the measured SINR is above a minimum value necessary for a correct detection. Otherwise, the message is lost and it is the responsibility of higher layers to detect and compensate this situation.
- eMBB throughput on the occupied resources: it measures the amount of data successfully transferred to the entire set of eMBB UEs over the used bandwidth. Note that the throughput is not a relevant performance indicator for RC traffic, which is characterized by small packets to be transmitted with a high reliability. In this study, it is only measured for the eMBB users. In particular, we aim at analyzing the eMBB throughput losses due to the usage of resources of multiple APs for serving the RC UE when multi-connectivity is activated.

#### A. Channel Measurement setup

The channel measurements are taken in two industrial scenarios, which we denote as Factory A and Factory B. The clutter in each scenario depends on the type of industrial machinery, as well as on the density of the installation. Factory A (Figure 3) has a reduced amount of clutter, with sparsely distributed light machinery, so line-of-sight (LOS) conditions for radio communication are more probable. Factory B (Figure 4) is a cluttered environment with heavy and large metallic machinery, packed in a dense layout, producing a higher probability of shadowing.

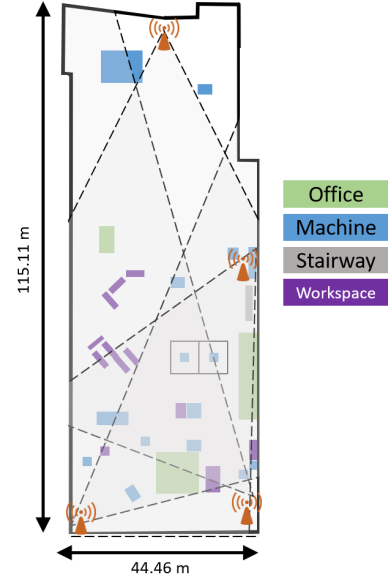


Fig. 3. Floorplan of Factory A with the AP positions.

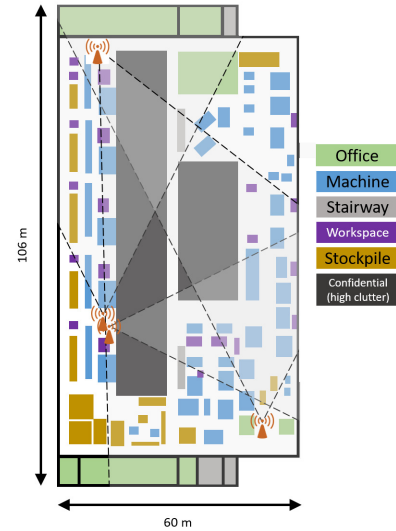


Fig. 4. Floorplan of Factory B with the AP positions.

Measurements have been taken by using an SDR testbed consisting of 12 nodes. 4 of them are configured as transmitters, and the other 8 nodes as receivers. Each node consists of 2 USRP RIO devices and a host PC that runs the measurement software. Figure 5 shows two of the SDR nodes. Each USRP device is considered as an independent terminal and has two RF chains enabling  $2 \times 2$  MIMO; that is, each testbed node has two co-located terminals. The node setup is mounted over a movable trolley to ease redeployments. The transmitter locations are deployed as shown in Figures 3 and 4. The receivers are distributed over 24 predefined positions via several redeployments. Panel antennas with  $60^\circ$  aperture are



Fig. 5. Nodes of the SDR testbed. The left image shows a transmitter node and the right image a receiver node.

used for the transmitter nodes, and omnidirectional dipole antennas for the receiving nodes. The transmit antennas are set at a 2.6 m height, while different heights per terminal are set for the receive nodes (1.75 m and 0.25 m, as shown in Figure 5). This is meant to emulate the diverse positions of industrial devices such as sensors and actuators in the factory environment.

Each transmitter generates a known signal, specifically a Zadoff-Chu sequence [18]. The Zadoff-Chu sequence is generated in the frequency domain and mapped over 600 subcarriers. The time domain signal is then generated via Inverse Fast Fourier Transform (IFFT) and repeated a number of times in order to fit a predefined slot duration. The system operates at a 3.5 GHz carrier frequency (which is the band that will be used in the future for industrial wireless networks [19]), and the transmission bandwidth is 18 MHz. The transmission of the Zadoff-Chu sequences is done by using a Time Division Multiple Access (TDMA) scheme with the approach shown in [12]. A frame structure with 4 slots is defined, where the transmission by the 4 transmitters are time multiplexed. This allows the receiver to discriminate the transmitter identity and the measured link. The receivers use the reference sequence to estimate the Channel Transfer Function (CTF) in the downlink. We refer to [12] for further details on the adopted measurement approach.

Table I summarizes the main radio parameters of the system. The outcome of the measurement campaign is a set of channel matrices representing the channel responses between the 4 transmitters and the 48 receiver locations (2 antenna heights per the 24 measurement positions).

### B. Emulation

The performance of multi-connectivity is analyzed via hybrid emulation, where the channel measurements taken in Factories A and B are replacing standard channel models. The scenario presented in Section III is used as a reference for the emulation. At each iteration of the emulation, four of the locations where the measurements have been taken

TABLE I  
RADIO PARAMETERS.

Frequencies	3.5 GHz
Modulation	OFDM
Reference sequence	Zadoff-Chu
Reference sequence length	601
FFT length	1024
Sampling rate	40 MS/s
Symbol duration	25 $\mu$ s
Signal bandwidth	18 MHz
Tx power	10 dBm
Antennas AP	1 Panel XP (2.6 m), 60° aperture
Antennas UE	2 dipole omnidirectional

are selected, representative of the 4 UEs. The role of the RC UE is assigned to a receiver of each of the selected locations in turn, and the rest of the receivers are assigned the role of eMBB UEs, resulting in four different scenarios per iteration. In each turn, an A/B testing is performed; first with only single connectivity and then with the different multi-connectivity options for the RC UE. In each case, the RC UE selects the serving APs; and the remaining APs are then serving the eMBB users. Once the assignments have been done, the CTFs measured by the UEs are used to obtain the downlink KPIs (SINR and throughput). The SINR is calculated according to the receiver type, by following the same approach as in [20], and then mapped to Shannon throughput. A single transmission stream (rank 1) per UE is assumed by the transmit nodes. This loop is repeated until all the possible location combinations are emulated.

The SINR of the RC UE depends on the specific multi-connectivity scheme, and is calculated as follows:

- SFN: the received signal is the superposition of the signal of the assigned APs (PN and SN), so the SINR will be calculated upon a modified CTF which is the complex sum of the two individual CTFs.
- JT: The channel-aware precoding allows for coherent combining of the signals generated by the APs at the receiver. The SINR will be the sum of the individual SINRs:  $SINR_{JT} = SINR_p + SINR_s$ , where  $SINR_p$  and  $SINR_s$  denote the SINR of the PN and SN, respectively. It is worth to mention that this reflects the ideal case of full channel knowledge at the transmitter, which may not be feasible in the practice; however, it represents an upper bound on the JT performance.
- HL duplication: since two separate packets are received, the one with the highest SINR will be chosen as the received packet. Therefore,  $SINR_{HL} = \max(SINR_p, SINR_s)$ .

Note that, for both SFN and JT, both signals coming from primary and secondary AP are useful signals. In case of HL duplication, packets are transmitted by the two APs in different time instants; that is, they would also suffer from their mutual interference, besides the interference from the other APs.



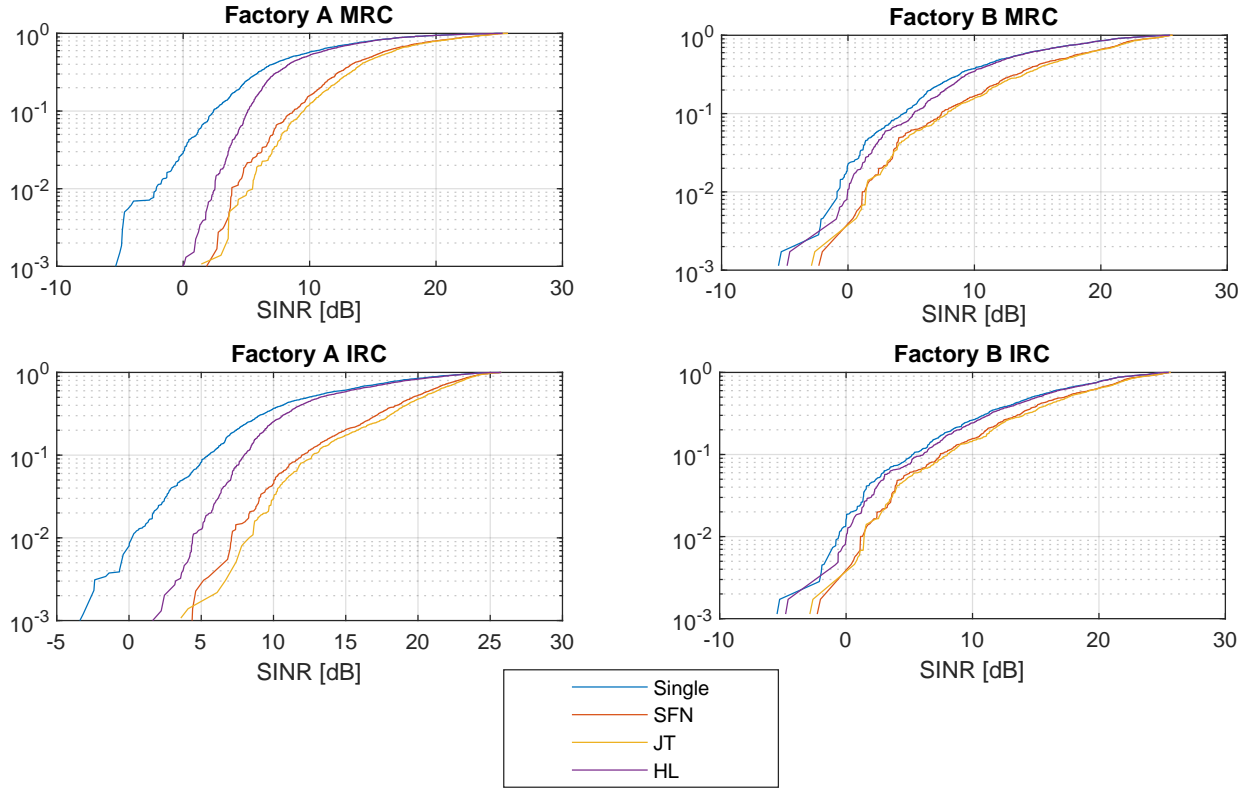


Fig. 6. ECDF of the measured SINR in the two scenarios.

#### IV. RESULTS

Figure 6 shows the Empirical Cumulative Distribution Function (ECDF) of the SINR of the RC UE in the two different scenarios and receiver types (MRC and IRC).

The multi-connectivity solutions (red, purple and yellow lines) clearly lead to a higher SINR gain with respect to single connectivity (blue line) in Factory A. In particular, the gain is in the order of  $\sim 8$  dB at a  $10^{-2}$  percentile for the physical layer multi-connectivity solutions compared to the  $\sim 1$ -2 dB gain in Factory B. By assuming for example a 0 dB SINR threshold for correct packet detection, in Factory A transmission appears to be successful for all the measured samples in case physical layer multi-connectivity is used, while in Factory B a remaining failure rate persists. The LOS conditions in Factory A cause indeed a high level of interference, leading to a significant performance improvement in case the strongest interfering link in single connectivity mode becomes a useful signal when multi-connectivity is used. In Factory B, on the other hand, the massive presence of obstructors protects the receiver from a high level of interference, diminishing the benefits of an additional useful link.

As expected, both SFN and JT clearly outperform HL duplication. As explained in Section III, this is due to the fact that in HL duplication, both primary and secondary AP still suffer from their mutual interference since they transmit the duplicated packets at different time instants. However, the

physical layer duplication improvements come at a significantly higher cost. It is worth to observe that no significant gain of JT with respect to SFN is visible. In this scenario, performance appears to be dominated by the instantaneous stronger link such that the benefits of signal combining enabled by JT are negligible.

The usage of an IRC receiver has a minor benefit with respect to MRC in Factory A (around  $\sim 2$  dB gain at the  $10^{-2}$  percentile), while its impact is negligible in Factory B. Given the two receive antenna terminals, IRC is able to suppress at most a single relevant interferer; the high amount of obstructors reduces the possibility of experiencing a relevant interferer in Factory B while this is more likely in Factory A, therefore leading to a higher gain in the latter scenario.

When activating multi-connectivity, some resources of the network are redirected to serve the RC UEs, so the resources available for eMBB are lower in that instant. Figure 7 shows the throughput of the eMBB users over the occupied resources of the network when the RC UE is served in single and multi-connectivity mode, averaged over all the instances of the emulation. The calculated throughput is the sum of the ideal Shannon capacity of each eMBB UE, based on the measured SINR and considering the total bandwidth of 18 MHz divided by the number of eMBB users served by the same AP. In both scenarios, the maximum throughput is about  $\sim 36$  % lower when comparing the multi-connectivity with respect to single connectivity. This is because in multi-connectivity, a

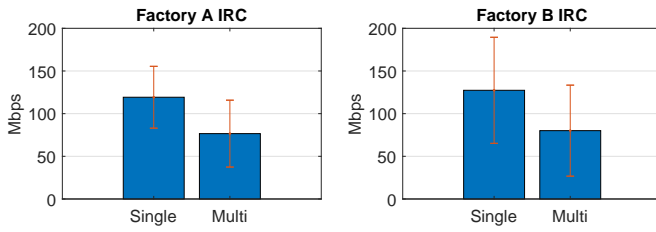


Fig. 7. eMBB throughput of the network in the assigned resources with single and multi connectivity.

second AP is dedicated to RC and the eMBB UEs can only choose between the remaining two APs. This increases the chances that the selected AP offers a lower receive power (and therefore a lower SINR) and that it is shared with other eMBB UEs; resulting in lower throughput. Figure 7 also shows a high standard deviation (represented by the thin red line). This is due to the high variability in the scenarios, caused by moving objects and the high variety of conditions found in the different locations where the measurement nodes were deployed. In Factory B the standard deviation is higher, responding to a higher clutter and movement of people and machines.

## V. CONCLUSIONS

In this paper, multi-connectivity has been studied as a solution for reliable communications. The analysis is based on a large set of channel measurements obtained in two industrial scenarios characterized by different amounts of clutter. Both physical layer and high layer duplication have been studied, considering multi-antenna Maximum Ratio Combining (MRC) and Interference Rejection Combining (IRC) receivers.

Multi-connectivity is shown to provide larger gains in the industrial scenario characterized by a low amount of clutter, given the dominance of LOS links which allow to convert relevant interfering links to useful signals. Minor benefits are instead visible in the scenario characterized by large shadowing levels. Physical layer duplication leads to the higher performance benefit, at the cost of additional implementation complexity with respect to packet duplication performed at a higher layer (e.g., PDCP).

Overall, multi-connectivity comes at a cost in the form of network throughput. Since resources are redirected to the UEs demanding reliable communication, a reduction in terms of eMBB throughput is observed.

## ACKNOWLEDGEMENTS

This research is partially supported by the EU H2020-ICT-2016-2 project ONE5G. The views expressed in this paper are those of the authors and do not necessarily represent the project views.

## REFERENCES

- [1] H. Lasi, P. Fettke, H.-G. Kemper, *et al.*, "Industry 4.0," *Business & Information Systems Engineering*, vol. 6, no. 4, pp. 239–242, 2014.
- [2] A. Al-Fuqaha, M. Guizani, M. Mohammadi, *et al.*, "Internet of things: A survey on enabling technologies, protocols, and applications," *IEEE Communications Surveys & Tutorials*, vol. 17, no. 4, pp. 2347–2376, 2015.
- [3] M. Series, "IMT vision—framework and overall objectives of the future development of IMT for 2020 and beyond," *Recommendation ITU*, pp. 2083–0, 2015.
- [4] V. Chandrasekhar, J. G. Andrews, and A. Gatherer, "Femtocell networks: a survey," *IEEE Communications Magazine*, vol. 46, pp. 59–67, September 2008.
- [5] P. Mogensen, K. Pajukoski, E. Tirola, *et al.*, "Centimeter-wave concept for 5G ultra-dense small cells," in *Vehicular Technology Conference (VTC Spring), 2014 IEEE 79th*, pp. 1–6, IEEE, 2014.
- [6] D. A. Wassie, G. Berardinelli, F. M. L. Tavares, *et al.*, "Experimental verification of interference mitigation techniques for 5G small cells," *IEEE Vehicular Technology Conference*, pp. 1–5, 2015.
- [7] D. A. Wassie, I. Rodriguez, G. Berardinelli, *et al.*, "Radio propagation analysis of industrial scenarios within the context of ultra-reliable communication," in *2018 IEEE 87th Vehicular Technology Conference (VTC Spring)*, pp. 1–6, June 2018.
- [8] J. Rao and S. Vrzic, "Packet duplication for URLLC in 5G: Architectural enhancements and performance analysis," *IEEE Network*, vol. 32, no. 2, pp. 32–40, 2018.
- [9] Y. Li, S.-H. Kim, B. L. Ng, *et al.*, "Methods and apparatus for inter-eNB carrier aggregation," Feb. 9 2016. US Patent 9,258,750.
- [10] M. Polese, M. Giordani, M. Mezzavilla, *et al.*, "Improved handover through dual connectivity in 5G mmWave mobile networks," *IEEE Journal on Selected Areas in Communications*, vol. 35, no. 9, pp. 2069–2084, 2017.
- [11] O. Tonelli, *Experimental analysis and proof-of-concept of distributed mechanisms for local area wireless network*. PhD thesis, Ph. D. thesis, 2014.
- [12] D. Assefa Wassie, I. Rodriguez, G. Berardinelli, *et al.*, "An agile multi-node multi-antenna wireless channel sounding system," *IEEE Access*, vol. 7, Jan 2019.
- [13] F. B. Tesema, A. Awada, I. Viering, *et al.*, "Mobility modeling and performance evaluation of multi-connectivity in 5G intra-frequency networks," in *2015 IEEE Globecom Workshops (GC Wkshps)*, pp. 1–6, Dec 2015.
- [14] P. Baier, M. Meurer, T. Weber, and H. Troger, "Joint transmission (JT), an alternative rationale for the downlink of time division CDMA using multi-element transmit antennas," in *Spread Spectrum Techniques and Applications, 2000 IEEE Sixth International Symposium on*, vol. 1, pp. 1–5, IEEE, 2000.
- [15] D. Lee, H. Seo, B. Clerckx, *et al.*, "Coordinated multipoint transmission and reception in lte-advanced: deployment scenarios and operational challenges," *IEEE Communications Magazine*, vol. 50, pp. 148–155, February 2012.
- [16] Y.-C. Chen, Y.-s. Lim, R. J. Gibbens, *et al.*, "A measurement-based study of multipath TCP performance over wireless networks," in *Proceedings of the 2013 Conference on Internet Measurement Conference, IMC '13*, (New York, NY, USA), pp. 455–468, ACM, 2013.
- [17] 3GPP, *NR and NG-RAN Overall Description*. 3rd Generation Partnership Project, TS 38.300 ed., December 2017.
- [18] M. M. U. Gul, S. Lee, and X. Ma, "Robust synchronization for OFDM employing Zadoff-Chu sequence," in *Information Sciences and Systems (CISS), 2012 46th Annual Conference on*, pp. 1–6, IEEE, 2012.
- [19] 3GPP, *Scenarios and Requirements for Small Cell Enhancements for E-UTRA and E-UTRAN (Release 12)*. 3rd Generation Partnership Project, TR 36.932 ed., December 2012.
- [20] D. A. Wassie, G. Berardinelli, F. M. L. Tavares, *et al.*, "Experimental evaluation of interference rejection combining for 5G small cells," in *2015 IEEE Wireless Communications and Networking Conference (WCNC)*, pp. 652–657, March 2015.